A new adaptive switching filter with directional impulse detection*

SUN Jing (孙菁)**, **LIU Hui-gang** (刘会刚), **and ZHANG Fu-hai** (张福海)
College of Electronic Information and Optical Engineering, Nankai University, Tianjin 300071, China

(Received 12 September 2013; Revised 4 December 2013)

A novel adaptive switching filter (ASF) based on directional detection is proposed for denoising the images that are highly corrupted by impulse noise. The proposed algorithm employs an efficient noise detection mechanism. It first employs an efficient method to estimate the differences between the current pixel and its neighbors aligned with 28 directions. The current noise pixel is replaced by a median or a mean value within an adaptive filter window with respect to different noise densities. Experimental results show that the proposed approach can not only achieve very low miss-detection ratio and false-alarm ratio even up to high noise corruption, but also preserve the detailed information of an image very well.

Document code: A **Article ID:** 1673-1905(2014)02-0157-4
DOI 10.1007/s11801-014-3162-3

There are many median filters, such as switching median filter (SMF)[1], adaptive median filter (AMF)[2,3] and noise adaptive soft switching median filter (NASMF)[4], for denoising images. Recently, an efficient decision-based algorithm (DBA)[5] has been proposed. However, they all perform well at low noise densities. Directional weighted median filter (DWMF)[6] and its improved algorithm (MDWM)[7] can work well for many natural images, but fail to incorporate many needed directions during impulse detection process for images with many details. The performance of switching median filter with boundary discriminative noise detection (BDND)[8] is good in detecting impulse noises with various densities. Based on Ref.[8], a highly effective impulse noise detection (HEIND) algorithm[9] was proposed. It provides an efficient method using both boundary based information and directional based information. This algorithm has a better ability in identifying impulse noise than the method in Ref.[8].

In this paper, a new adaptive switching filter (ASF) based on directional detection is proposed. It employs the differences between a center pixel and its neighboring pixels aligned in 28 directions. The simulation results show that the proposed algorithm can achieve excellent performance in a wide range of noise densities.

We focus on the salt-and-pepper impulse whose pixels are randomly corrupted by two fixed extreme values, 0 and 255 (for 8-bit monochrome image), generated with the same probability[10]. Assume the size of a noise-corrupted image is $M\times N$. First, a noise-corrupted image is analyzed by an extrema detection mechanism. If the value at location (i, j) is an extreme value (0 or 255), the current pixel is classified to a suspicious noise. An estimated noise density is obtained as R_1:

$$R_1 = \frac{\text{number of suspicious noise pixels}}{M\times N}, \tag{1}$$

where R_1 is used to decide the noise-filtering method.

Second, the 28 directional detection mechanism is operated to decide whether the suspicious noise pixel is a real noise pixel or not. Traditional direction-based noise detections only consider the differences between center pixel and its neighboring pixels within some single directions, ignoring the situation that the current pixel may be an inflection point of one edge. In order to improve the detection accuracy, 28 directions are employed to detect the edge direction of an object. Fig.1 shows the 28 directions for edge detection at location (i, j). The pixel at location (i, j) is a suspicious noise decided by the extrema detection mechanism.

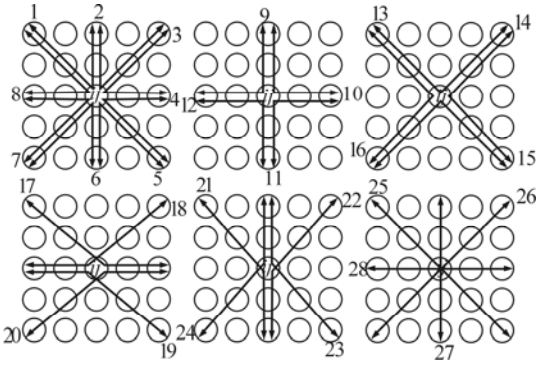

Fig.1 28 directions for edge detection

* This work has been supported by the Natural Science Foundation of Tianjin (No.13JCQNJC01200).
** E-mail: bluestarco@sina.com

As shown in Fig.1, to a 5×5 window centered at (i, j), for each direction, we compute the absolute differences of gray-level values $D_{i,j}^{k}$ between the center pixel $X_{i,j}$ and its neighbors $X_{i+s,j+t}$, for $1 \le k \le 28, (s,t) \in [-2,2]$. $D_{i,j}^{k}$ is given as

$$D_{i,j}^{k} = \sum_{s} \sum_{t} | X_{i+s,j+t} - X_{i,j} | \quad . \tag{2}$$

Considering the correlation between pixels, the gray-level values should be close when they are the edge of an object or in the same smoothly varying area. The minimum absolute difference of the 28 direction $D_{i,j}^{km}$ is selected to be the most closely allied direction for the edge. $D_{i,j}^{km}$ can be expressed by

$$D_{i,j}^{km} = \min(D_{i,j}^{k}),\ 1 \le k \le 28 \, . \tag{3}$$

In order to find the minimum absolute difference $D_{i,j}^{km}$, there is no need to calculate each absolute difference of the 28 directions with Eq.(4). Making use of combination theory can decrease the computations and increase efficiency. As shown in Fig.2, the absolute difference $d_{i,j}^{l}(1 \le l \le 8)$ of eight simple directions is firstly computed. Then these eight values are arranged in ascending order V_D. We select two minimum values $d_{i,j}^{lm1}$ and $d_{i,j}^{lm2}$ $(lm1, lm2 \in \mathrm{l})$ of V_D and add them together. It is necessary to state that these two minimum values do not contain zero value for the purpose of eliminating the effect of one direction with the same noise pixels. This computation strategy can be expressed as follows:

$$D_{i,j}^{km} = d_{i,j}^{lm1} + d_{i,j}^{lm2},\ d_{i,j}^{lm1}, d_{i,j}^{lm2} \ne 0 \, . \tag{4}$$

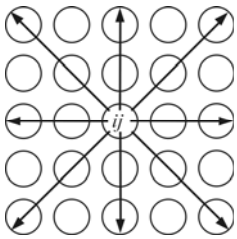

Fig.2 8 directions for combination

$D_{i,j}^{km}$ is used to detect whether the center suspicious noise pixel of a local window is noisy or noise-free, and the impulse detector can be defined as

$$X_{i,j} \in \begin{cases} \text{noise pixel}, & \text{for } D_{i,j}^{k} > T \\ \text{noise-free pixel}, & \text{others} \end{cases} , \tag{5}$$

where T is a predefined threshold value.

According to Eq.(6), whether the center pixel of a local window is a real noise or not is decided. After that, the noise density R_2 is recalculated to decide the maximum size filtering window. R_2 is defined as

$$R_2 = \frac{\text{number of real noise pixels}}{M \times N} \, . \tag{6}$$

Finally, a new type adaptive noise-filtering mechanism is employed in the proposed algorithm. If the center pixel is classified to be noise-free, it should be kept unchanged. Conversely, if the center pixel is classified to be noisy, two ways will be used to remove it. Before the process of noise filtering, R_n, R_{N1} and R_{N2} are predetermined as threshold values to compare with R_1 and R_2. Our filtering rule is as follows.

(1) If $R_1 \le R_n$, the size of filtering window is set to 3×3, as shown in Fig.3. Because the center pixel of a local window is always related closely to pixels close to it, the noise pixel is replaced preferentially by the median value of noise-free pixel values with closer distance (defined as 1). If the pixels closer to current noise pixel are all classified to be noisy, the noise pixel is replaced by the median value of noise-free pixel values with longer distance (defined as 2).

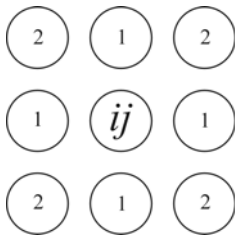

Fig.3 The distance of pixels within 3×3 filtering window

(2) If $R_1 > R_n$, the noise-filtering mechanism will choose mean values to replace noise pixels. Because most of the information of a corrupted image with higher noise density is covered by noise, the center pixel weakens its link to its neighboring pixels. Experimental results show that the mean value of noise-free pixels can reach better effects than the median value. The maximum size of filtering window $W_{\max}$ is set as follows:

$$W_{\max} = \begin{cases} 3\times 3, & \text{for } R_2 \le R_{N1} \\ 5\times 5, & \text{for } R_{N1} < R_2 \le R_{N2} \\ 7\times 7, & \text{for } R_2 > R_{N2} \end{cases} . \tag{7}$$

For images with different noise densities, the filtering window starts with 3×3, and iteratively extends outward by one pixel in all the four sides. If there are noise-free pixels in current window, the center noise pixel is replaced by the median value of them. Otherwise, the filtering window will be extended by one pixel outward until $W_{\max}$.

To ensure high accuracy of filtering, the proposed filter is performed iteratively for K times.

To demonstrate the effectiveness of the proposed algorithm, restoration results are compared with those of four representative state-of-art algorithms: MF (5×5 filtering window), AMF (3×3 to 5×5 filtering window), BDA and BDND. Two gray scale images of Man and

Woman with their resolution of 512×512 are selected to test the performance, as shown in Fig.4. In the simulation, the test images are corrupted with salt-and-pepper impulse noise. The noise density ranges from 10% to 90% with increment of 20%. The performance evaluation of the filtering operation is quantified by miss-detection ratio (MDR), false-alarm ratio (FAR), peak signal-to-noise ratio (PSNR) and running time (RT). MDR, FAR and PSNR are defined as follows respectively:

$$MDR = \frac{\text{number of miss detection noise}}{\text{number of total noise}}, \tag{8}$$

$$FAR = \frac{\text{number of false alarm noise}}{\text{number of total noise}}, \tag{9}$$

$$PSNR = 10\log 10\left(\frac{255^2}{MSE}\right)\text{dB}, \tag{10}$$

$$MSE = \frac{1}{M \times N}\sum^{M}\sum^{N}(Y_{i,j} - X_{i,j})^2, \tag{11}$$

where $M\times N$ is the total number of pixels in the image. $Y_{i,j}$ and $X_{i,j}$ denote the pixels of the restored image and original image, respectively.

(a) (b)

Fig.4 Testing images we used: (a) Man; (b) Woman

Our experimental results show that when T=5, R_n=0.4, R_{N1}=0.4, R_{N2}=0.7, and K=5, the proposed algorithm can achieve a better result. Computer simulations in Matlab 2010b are carried out to assess the performance.

The MDR and FAR values of Man and Woman from different filtering techniques are shown in Tab.1. It can be seen that the proposed method has an extraordinary ability in identifying impulse noise, and it can achieve low miss-detection ratio and false-alarm ratio. Comparisons of the values of PSNR with various algorithms are presented in Tab.2. The simulation results show that at all noise densities, PSNR values of MF, AMF, BDA and BDND are lower than that of ASF. Though ASF uses an iterative filtering method, it first operates an extrema detection to the updated image, which makes the computation reduced greatly for each time. As shown in Tab.3, the RT of ASF is much less compared with BDND, although it is more than others, so it can reach better filtering results.

In order to compare the performance subjectively, results of the filters are shown in Figs.5-7. It is obvious that the proposed filter performs better.

Tab.1 MDR and FAR of DBA, BDND and ASF filtering techniques

(a) Man

Noise	DBA		BDND		ASF	
density	MDR	FAR	MDR	FAR	MDR	FAR
10%	0	1.21	0	0	0	0
30%	0	0.15	0	1.28×10^{-5}	0	0
50%	0	3.12×10^{-2}	0	0	0	0
70%	0	6.57×10^{-3}	0	2.72×10^{-5}	0	0
90%	0	1.01×10^{-3}	0	1.25×10^{-3}	0	0

(b) Woman

Noise	DBA		BDND		ASF	
density	MDR	FAR	MDR	FAR	MDR	FAR
10%	0	1.38	0	3.56×10^{-2}	4.94×10^{-4}	1.45×10^{-2}
30%	0	0.18	0	9.52×10^{-3}	3.69×10^{-4}	4.58×10^{-3}
50%	0	3.91×10^{-2}	0	4.9×10^{-3}	2.68×10^{-4}	2.93×10^{-3}
70%	0	2.48×10^{-3}	0	3.31×10^{-3}	1.42×10^{-4}	1.93×10^{-3}
90%	0	1.06×10^{-3}	0	2.59×10^{-3}	4.67×10^{-5}	1.37×10^{-3}

Tab.2 PSNR(dB) of different filtering techniques

(a) Man

Noise	MF	AMF	DBA	BDND	ASF
10%	28.39	35.26	35.19	40.25	40.96
30%	27.34	31.68	31.57	34.39	34.69
50%	23.34	28.24	28.17	30.59	31.38
70%	14.11	22.60	25.02	27.34	28.47
90%	7.49	10.29	20.27	24.03	24.53

(b) Woman

Noise	MF	AMF	DBA	BDND	ASF
10%	37.73	44.44	44.32	48.47	49.22
30%	35.65	40.01	39.90	42.44	43.00
50%	25.42	34.83	35.82	38.22	40.35
70%	14.09	22.92	31.68	34.62	36.61
90%	7.15	9.99	24.42	30.14	31.78

Tab.3 RT(s) of different filtering techniques for Man

Noise	MF	AMF	DBA	BDND	ASF
10%	0.09	0.40	5.54	12.48	4.57
30%	0.09	0.40	5.44	16.26	12.51
50%	0.09	0.41	5.47	20.33	5.56
70%	0.09	0.43	5.45	25.05	7.71
90%	0.09	0.40	5.57	29.79	11.12

(a) (b) (c)

(d) (e) (f)

Fig.5 Image restoration results of the Man image with different techniques: (a) 70% noise corrupted; (b) MF; (c) AMF; (d) DBA; (e) BDND; (f) ASF

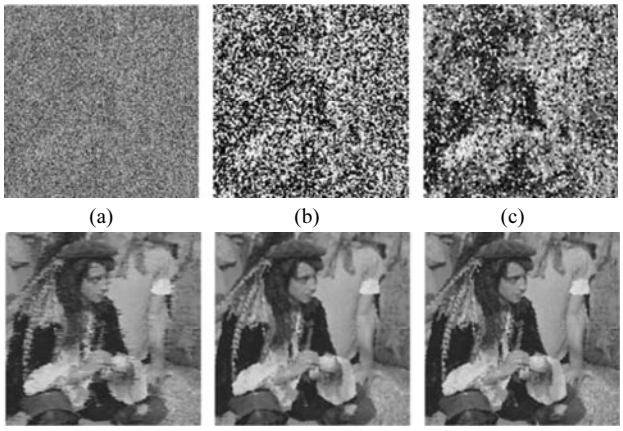

(a) (b) (c)

(d) (e) (f)

Fig.6 Image restoration results of the Man image with different techniques: (a) 90% noise corrupted; (b) MF; (c) AMF; (d) DBA; (e) BDND; (f) ASF

(a) (b) (c)

(d) (e) (f)

Fig.7 Image restoration results of the Woman image with different techniques: (a) 90% noise corrupted; (b) MF; (c) AMF; (d) DBA ; (e) BDND; (f) ASF

Objective and subjective experimental results show that ASF performs better than other existing denoising techniques.

References

[1] T. Sun and Y. Neuvo, Pattern Recognit. Lett. **15**, 341 (1994).

[2] H. Hwang and R. A Haddad, IEEE Trans. Image Process. **4**, 499 (1995).

[3] R. C. Gonzalez and R. E. Woods, Digital Image Processing, 2nd ed., Upper Saddle River, NJ: Prentice Hall, 2002.

[4] H. L. Eng and K. K. Ma, IEEE Trans. Image Process. **10**, 242 (2001).

[5] K. S. Srinivasan and D. Ebenezer, IEEE Signal Process. Lett. **14**, 189 (2007).

[6] Y. Q. Dong and S. F. Xu, IEEE Signal Process. Lett. **14**, 193 (2007).

[7] C. T. Lu and T. C. Chou, Pattern Recognit. Lett. **33**, 1287 (2012).

[8] P. E. Ng and K. K. Ma, IEEE Trans. Image Process. **15**, 1506 (2006).

[9] F. Duan and Y. J. Zhang, IEEE Signal Process. Lett. **17**, 647 (2010).

[10] I. Pitas and A. N. Venetsanopoulos, Nonlinear Digital Filter: Principles and Application, Kluwer, Boston, MA, 1990.